ANALYSIS OF THE INFILTRATION COMPLEX SYSTEM USING A NOVEL GSA-HYBRID FOR AUTOMATIC CALIBRATION FOCUSED AT CIVIL CONSTRUCTION

Domingo-Stalin Aguero-Martinez [1]
ORCID**:** 0000-0003-0620-9318

Thiago Barros Murari [1]
ORCID: 0000-0001-5598-2679

Marcelo Albano Moret [1]
ORCID: 0000-0003-0051-6309

[1] University of Senai-Cimatec, Brazil.
* Correspondence: domingostalin@ifba.edu.br

Abstract:

Among the various complex systems that we experience each day, there is the physical phenomenon of infiltration. Infiltration is considered as the dynamics of water flow in the subsurface soil that in this work is framed for the context of civil construction. This issue is approached with the use of mathematical models and stochastic techniques, however, there are hardships in collecting the samples in the field, the adoption of a scale type, the influence in soil layers' interfaces, the effects of soil anisotropic characteristics and so on. In this study, methodology is proposed to deal with the soil sampling input such as the retro model, constitutive model and optimization algorithms. Additionally, an automatic calibration is set forth to fix parameters from the mathematical model submitted. Especially among the existing Optimization Algorithms there are Genetic Algorithms and the Generalized Simulated Annealing Algorithm (GSA). This work presents an overview of these optimization methods and a proposal for a more efficient and faster algorithm called GSA-HYBRID based on convergence gradient technique. The applied strategy depends on the type of case study considering its physical properties and constraints. In this sense, it is found that while Genetic Algorithms are able to replicate the optimization surface, Generalized Simulated Annealing is much more adequate in characterizing the system at an extremely low computational cost. Nevertheless, the hybrid technique GSA-HYBRID performed the fastest. Further research is necessary to implement the novel GSA-HYBRID algorithm due to its flexibility and higher speed, also, studying its application at different case studies.

Keywords:

Infiltration, GSA-HYBRID Algorithm, GSA Algorithm, Genetic Algorithms, Calibration, Characteristic Curve.

---

1. Introduction

Complex systems circumvent our daily life and activities, such as temperature, weather, wind, electricity, light, rain and water infiltration. These factors, even in well-planned civil construction, have always been the cause of serious pathologies and large expenses for the construction industry. In particular, understanding about water infiltration in the soil helps in supporting the possible assessments and/or decision-making of managers in different fields such as irrigation, urban drainage networks, agriculture and so on [1-4].

The physical phenomenon of infiltration is based on the dynamics of the volumetric content of water, which in turn is related to the flow of water in the unsaturated zone. Whereas, the study of this physical phenomenon is complicated due to the hamper to obtain unsaturated soil samples called in this work as "observed data". These samples are located underground and hard to reach without changing their natural conditions [5]. Therefore, to contour this problem several instruments were developed such as the Time Reflectometry Techniques (Time Domain Reflectometry - TDR) which have the advantages of not destroying the sample and not perturbing the front of the soil moisture advance. Nevertheless, other types of problems seriously affect the field collected data such as the type of scale and the interfaces of different layers of soil.

Larger scale and several layers of soil hamper the simulation of the physical phenomenon of infiltration. In particular, the moisture advance front suffers disturbances at the interface of soil different layers due to the low values of unsaturated soil hydraulic conductivity. On the other hand, sensitivity of parameters increases as large scale experiments with different soil layers are approached, complicating the automatic calibration and, consequently, increasing the difficulty to obtain simulated parameters results [6].

In addition, anisotropic soil affects infiltration study due to heterogeneous properties depending on the location of the water table and the variability of the region of the unsaturated zone. Soil heterogeneity influences on numerical calculations continue to be studied hitherto, some conclusions indicate that regardless of whether the soil is heterogeneous or not, at a certain depth, the volume of water infiltrated follows a growing power law while the infiltration rate follows a decaying power law [4]. To circumvent these difficulties, in this work, a smaller scale experiment is characterized. In this situation, the soil is considered homogeneous and well classified, with well-characterized hydraulic properties considering only one layer of soil. Therefore, noise or uncertainty is reduced as much as possible, which would facilitate the verification of results of simulation of the infiltration phenomenon [7].

Regarding the modeling of infiltration phenomenon, a partial differential equation called "Richards equation" was established that describes the infiltration process, however, it is emphasized that it is a highly non-linear function with the paradox that the parameters are in function of the variables [8–10]. Richards equation solution simulates appropriately parameters values of water content and matric potentials. As aforementioned, these parameters values are hampered to obtain in the field due to being in subsurface regions as compared to the facility to collect superficial zone data. In order to assist in solving Richards equation heuristic mathematical models were adopted such as the constitutive models and the inverse model [11–12].

Constitutive models began by associating both volumetric moisture and the matric potential of unsaturated soil in an experimental model called "pressure disc

effluent method". In this model, air pressure is added to a saturated soil sample so measuring the respective effluents. Then, the so-called soil water retention curve, or also known as the characteristic curve, was established [13]. These studies progressed to the point of developing several correlations of characteristic curves with their respective heuristic equations being the van Genuchten model, one of the most recognized in literature and it is used in the present work [14, 4].

As mentioned earlier, another mathematical model of dealing with solving Richards equation is the retro model or inverse model. This approach consists of submits initial model parameters values arbitrarily to the mathematical model proposed until reaching as output the calculation of parameters and as a consequence the simulation of the infiltration phenomenon. This technique is well recognized in the literature, Ramos et al. [15] used this technique for three types of soil comparing the characteristic curves. These characteristic curves are based on input data obtained from infiltration tests and, also, with data acquired in the laboratory, obtaining reasonable convergence. Papafotiou et al. [16] evaluated the hydraulic properties of the sand applying the inverse model at a multi-step effluent experiment obtaining reasonable criteria of approaching methods as pore scale and lab scale.

Whereas, these soil water retention equations were studied unidimensionally using the Philips Infiltration Model being the first analytical solution of the Richards equation, helping to elucidate not only the water flow in unsaturated soil but also the sorption process [17–18]. Regardless, it is hamper to validate these Philips model results for 3D simulations due to the complexity of the system, the scarcity of good laboratories or field data and the lack of knowledge related to hydraulic properties. It should be noted that in order to achieve the real study of a complex system, it is imperative to contextualize this complex system layout in spatial dimensions and not limitedly as it was initially considered as a unidirectional gravitational phenomenon [3–4].

The correlation adjustment that exists among issues such as the highly non-linear equation, parameters, variables, collected data, all of these confined in a hypercube in which the imposed mathematical model acts, needs a complex calibration technique. Over the years, it has been found that the calibration techniques in the aforementioned models upheld intense research in the literature, starting from manual calibration till to the advent of electronic computers that enhanced the automatic calibration. Following this line of research for automatic calibration, it was noticed that several authors adopted stochastic algorithms in adjusting the model to reach the global optimum being Genetic Algorithms one of the pioneers [19–21].

The concept of Genetic Algorithms began in the field of biology starting from the premise of evolution and sketching how a living being adapts to its environment over generation. A simple artificial adaptive system is designed to simulate a complex or non-linear natural adaptive system through a formal structure and accurate operators. Complex genetic systems (phenotypes) have a structure based on chromosomes and mutation operators that recombine functioning as alleles. Control and optimization of a function was conceived as an artificial central nervous system and adaptive agents (economy, political systems, ecology, immune system). It was focused on schemata ideas and the location of an optimum value through learning (trial and error) and artificial intelligence (random search). Genetic Algorithms work with people and for that purpose different types of genetic operators were incorporated into their reproductive plan such as the crossing, the inversion and the mutation [19–20].

Over the years, Genetic Algorithms - GAs were applied to engineering such as the pipeline industry [21]. GAs were improved in terms of the best performance in a

reasonably limited time by developing other types of operators, such as the roulette technique and so on. Improving random criterion was a main feature to efficiently explore the historical information of successful results to speculate on new points with the expectation of a better performance. Additionally, Genetic Algorithms are distinguished by the characteristic of being robust in the search for the global optimum through random searches [21].

Genetic Algorithms – GAs were applied to urban water drainage to understand the behavior of hydrodynamic models adopted for the quantification of risk in urban drainage systems given the seasonality of a critical rain event [22]. In these case studies, GAs have been improved especially in the use of random operators to compute and recombine chromosomes to generate new improved entities in the purpose of adjusting the model. When compared to other optimization algorithms, GA presented a better performance in obtaining a better adjustment of the parameter values using a smaller number of iterations and taking a lower computational cost. It is emphasized that heavy meta-heuristic concepts are inherently embedded as the complexity of the model increases or the types of optimization algorithms enhance or the computational power intensity, however, the system analysis also is improved [22].

Genetic Algorithms were used in the hydrological and agricultural fields. In these issues, GAs was associated with Philip's infiltration model by studying the infiltration phenomenon in the vertical direction. The criterion of disturbance series around the sorption process was used in the model equation of two infiltration terms of Philip, thus defining the parameterization of the model to be calibrated. However, Philip's model, despite being appreciably recognized in the literature, is confined to the unidirectional state, and thus, does not conceive the reality of the complex system of the infiltration phenomenon [9].

Genetic Algorithms were used to calibrate the sedimentation phenomenon, using finite volumes, adjusting an objective function of least squares between observed and simulated data. For that purpose, the water flow transport equation was applied which is characterized by its high non-linearity. The concentration of solids over time was determined and the water flow over time was considered the main parameter [23]. A variant of the traditional technique of Genetic Algorithms has been proposed, called Continuous Genetic Algorithms, which fits into a great application for synthetic data [23].

Genetic Algorithms (GAs) were used for calibration in water supply systems to optimize energy costs. The model was a larger scale case of study located in the city of Ourém (Portugal). GAs performed a decrease in computational time in relation to other models [24]. Afterwards, we propose the use of the stochastic strategy for the adjustment of parameters based on the Generalized Simulated Annealing - GSA and we discuss its application in different fields of science.

The GSA concept initiated in understanding the connection between statistical mechanics, that is, the behavior of systems with many degrees of freedom that reach thermal equilibrium at a freezing temperature, and combinatorial or multivariate optimization [25]. An example of statistical mechanics can be found in annealing (metals) which, in order to determine the lowest state temperature of a material, must be carefully annealed, so it is similar to the optimization problem [25]. The availability of an appropriate temperature to the system leads to a simulated annealing process being favorable in obtaining heuristic solutions to the optimization problem. The iteration technique improves as per the microscopic rearrangement process modeled by statistical mechanics and considering the minimization of energy as a cost function.

To avoid rapid cooling, the Metropolis technique [26] provides an efficient simulation considering the set of atoms in equilibrium and a given temperature, achieving the simulation of annealing. As per this procedure, each step of the algorithm is equivalent to an arbitrary displacement of the atom with resulting changes in the objective function or energy of the system. If the good-of-fitness of the cost function is less than the previous value then it is accepted as a new value, however, when the calculated value is greater than the previous one it is accepted with the probability determined by the Boltzmann distribution. This annealing procedure using temperature as a parameter of the cost function or energy system reaching different levels of temperature equilibrium as per this arbitrary displacement of atoms until reaching the rearrangement of atoms to a minimum temperature was called the Classical Simulated Annealing (CSA) or the Boltzmann machine [26].

The method was submitted to two situations which are the physical design of computers and the classical problem of the "Travelling Salesman Problem". In both cases, problems were addressed in connection with two philosophical concepts: "divide and conquer" and progressive iteration. In the first concept, the whole domain is divided into subsystems in order to execute the algorithm in each sub-system and, if successful, progress to other subsystems until reaching the global optimum. In the second, if there is an improved system, rearrangement should restart the iteration based on the best vector response sum of some great location and, thus, continue the iteration progressively till achieving the absolute minimum of the objective function [26].

The GSA algorithm was improved when a Cauchy-Lorentz visitor distribution was used instead of the Gaussian visitor distribution, a procedure known as Fast Simulated Annealing (FSA) [27]. This technique performs a semi-local search consisting of occasional long jumps. Another feature of this technique is that the cooling process of the FSA algorithm is inversely linear over time, which is fast compared to classic simulated annealing (CSA), which is strictly a local search and requires that the cooling process is inversely proportional to the logarithmic function of time. This technique was called the Cauchy machine [27].

However, the simulated annealing procedure was generalized for the two distributions already mentioned, that is, the Gaussian visit distribution of Boltzmann-Gibbs (Boltzmann machine) and the Cauchy-Lorentz visit distribution (Cauchy machine). Both anneals were framed in the generalized statistical mechanics following the Tsallis statistic called the Tsallis machine. Thus, the proposed technique was called the Generalized Simulated Annealing (GSA) [28–30].

An analytical way was proposed to obtain the parameters of GSA algorithm using numerical integration. This increased the speed of the optimization algorithm compared to conventional methods Boltzmann machine and Cauchy machine [30].

In recent years, other advances have been developed in the GSA algorithm, like, qT parameter was independent of the other parameters qA and qV being three parameters. In addition, the visitation iteration advance step was calculated directly from the visitation distribution function instead of integrating it numerically. Furthermore, a hybrid convergence was proposed which holds the GSA response close to an optimum, subsequently, it is applied a gradient descent method so reaching the value of the optimum no matter local or global [31–32].

Higher speed and adaptability characteristics makes GSA being profitable to analyse unsaturated water flow as proposed in this work. Furthermore, this work adapts a conjugate gradient technique to GSA in order to analyse its effects and compare its results versus other optimization algorithms. Problems of infiltration

treated with GSA algorithm were not reported hitherto, however, applied to other fields of science proved to be efficient and being extremely fast.

GSA was utilized to optimize structure of molecules and macromolecules in which energy surface minimum values were obtained from a classical force field. Modified GSA using numerical integration lasted a few minutes to obtain simulated values being faster than traditional GSA took time of days [30].

GSA was employed in the field of biology particularly at molecular dynamics being compared to other techniques such as metadynamic and replica-exchange. Consequently, the system was well characterized by GSA with the expenditure of a reasonable amount of time [33].

GSA was used in the field of chemistry to analyze the stability of Kr-CH3OH (Krypton-Metanol) complex considering electrostatic interactions and intermolecular theories. For this study, rotation-vibration method performed a relevant role where a parameter called "sized parameter" was optimized. For that, simplex gradient and Levenberg-Marquardt methods were implemented in GSA. Using these tools, it was concluded that Krypton-Metanol is stable [34].

Again, in the field of biology, GSA technique was employed to determine tridimensional structure of protein. Inverse GSA visit function and minimization of energy techniques were used in the process. This represented a great advance to choose computational techniques instead of experimental methods. Computational methods just require previous structures resulting in less expensive than traditional experimental methods [35].

In the field of chemistry, hybrid procedures (GSA, Simplex gradient and Levenberg-Marquardt) were utilized to optimize Rydberg function coefficient. On the way, rotation-vibration energy levels, electroscopic constants and dynamic properties were calculated. This system was based on Density Functional Theory (DFT) and the nuclear equation of Schrödinger using a variable discrete representation to model interaction between ammonia and metallo-phthalocyanines aiming at chemical sensory design [36].

In the field of physics, GSA was modified and employed to determine a double zeta input atomic new base for electronic calculation of Li and Be. To this, an electronic atomic energy function was optimized. It performed a fundamental state energy calculation of the Be atom in order to test new bases with reasonable results between input and output [37].

After this review of literature about optimization algorithms and its application and showing the art-of-state of infiltration complex systems, we established the predominant objective of this work which is unsaturated water flow analysis. Secondary objectives are: understand the function of Optimization algorithms and to obtain a better comprehension of physical properties of the case of study considering the unsaturated water flow infiltration physical phenomenon. We establish the north question: Is it possible an optimization algorithm capable of simulating the physical phenomenon of infiltration obtaining reasonable parameters in a lower computational cost?

This work is organized in section two methodology describing equations of unsaturated water flow and optimization algorithms. Also, section two presents the case of study, hypotheses and constraints. Then, infiltration experiment inputs are shown. Section three performs a discussion of infiltration simulation output. Afterwards, section four presents conclusions and, at last, literature references.

2. Methodology

Methodology begins describing optimization algorithms. Afterward, a case study was described. And, at last, a mathematical model and its interaction with optimization algorithms to simulate the physical phenomenon was established.

2.1 Optimization Algorithms: Genetic Algorithms and Generalized Simulated Annealing

2.1.1 Genetic Algorithms

Genetic Algorithms - GAs emulate evolution through natural selection and reproduction, therefore, natural selection determines survivors to reproduce and the term of reproduction indicates the idea to combine genes of herders. GAs is considered a binary system of a chain of bites where string *1* means right and string *0* means wrong. One entity is represented by a bit of chain as a result of a computational process; if binary suffers a combination of bits another entity would be represented. In other words, GA ability is based on elaborate partial responses to improve it for combined bits in computational terms [19-20].

Another advantage of Genetic Algorithms is based on the facility to manage its binary codification, avoiding several limitations (such as being continuous, existence of derivative, unimodal, and so on) imposed by other optimization techniques. On the other hand, GAs character chains can work in parallel following several ways to reach a solution avoiding false optimum.

Furthermore, the benefit of Genetic Algorithms depends on construction of characters and population using a random "seed", for instance, flipping a coin determines head code *1* and tail code *0* and thereby creating future generations.

Genetic Algorithms do not require other auxiliary techniques, such as gradient descent that demand derivative methods. Only condition to good-of-fitness is an objective function that works in connection with population generated automatically. The fitness value of objective function is the metric of fitness process [21].

Thereby, robustness in Genetic Algorithms is characterized by four requirements: first, codification in characters; second, random population; third, do not use auxiliary information meaning "blind search"; fourth, random operators. In this last requirement about random operators were defined the following operators: reproduction, crossover and mutation [21].

Reproduction performs a copy of character binary chain that better fitness objective function. In that way, Genetic Algorithms reproduce "offspring", in other words, to generate a population of binary chains with a great chance to reach the global optimum. Tendentious roulette wheel was used to exemplify the manner to reproduce individuals where slots are dimensioned as per the fitness of each individual. Thereby, each reproduction candidate individual is chosen as per the spin of the roulette wheel forming a partial population constituted of possibly more individuals reproduced by the roulette bigger slot. Those partial populations reproduced individuals that are mating in pairs selected randomly from all reproduced individuals (mating pool) [21].

Subsequently, crossover operators act by arbitrarily dividing both mating individuals and switching those divided parts. As a result, mating individual processes and applying crossover operators eliminate "feeble" individuals developing robustness quality for Genetic Algorithms [21].

Nevertheless, it is possible no convergence to the optimum value, in that case, another operator called mutate is applied. Mutation performs the substitution of a tiny part in a random manner (with little probability) switching the value of a bit from the whole bit chain. It means, switch the value of bit *0* by bit *1*, and vice versa, this process is done occasionally and considered a secondary mechanism of adaptation [21].

To this moment, it was discussed about robustness of Genetic Algorithms -GAs techniques searching the optimum global such as random initial parameters called seed, using an objective function, converting in binary code those arbitrary parameters and invoking probabilistic operators [21]. Over the years, GAs was used in different fields of science and received several modifications.

In the field of medicine, Genetic Algorithms were used to optimize laser systems using advanced operators such as: tournament, jump, elitism, uniform crossover or singular point, creep, niching and so forth. From all of these operators, Elitism operators stand out that force the partial optimum individual obtaining the best good-of-fitness from the objective function. This partial optimum individual remains till another best individual appears [38].

It was upheld that a population of five individuals avoids premature convergence and performs a fast convergence near the global optimum region called micro-GA technique of Krishnakumar [39]. Those criteria of Genetic Algorithms are used in this work as well as the concept of micro-GA technique.

2.1.2 Generalized Simulated Annealing Algorithm

As previously stated, Generalized Simulated Algorithm is considered in this work to approach the study of infiltration phenomenon. As aforementioned about origins of GSA, issues such as the Boltzmann machine, sequentially, the Cauchy machine and at last a combination of both called the Tsallis machine [25–29] were implemented. Therefore, some tools established for GSA methodology are: generalized acceptance probability, Metropolis algorithm [26], acceptance temperature that decreases over time, Tsallis statistical distribution, and so on. Afterwards, methodology focus to determine variable value x_t to obtain a next variable value x_{t+1} ($x_t \dashrightarrow x_{t+1}$) resolving visiting distribution $g_{qv}(\Delta x_t)$ being ($\Delta x_t = x_{t+1} - x_t$) and qV visiting parameter. For D dimensions and qV=1 it is established $g_1(\Delta xt) = \dfrac{e^{-(\Delta xt)^2/T_1^v(t)}}{[\pi T_1^v(t)]^{\frac{D}{2}}}$ being $T_1^v(t)$ visiting temperature over time *t*. For qV=2 visiting distribution is $g_2(\Delta xt) = \dfrac{T_2^v(t)}{[[T_2^v(t)]^2+(\Delta xt)^2]^{\frac{D+1}{2}}}$ being $T_2^v(t)$ visiting temperature over time *t*. This last expression can be enhanced using Fourier Transformation over D dimensions resulting:

$$g_2(\Delta xt) = \frac{\Gamma\left(\frac{(D+1)}{2}\right)}{\pi^{\frac{(D+1)}{2}}} \frac{T_2^v(t)}{\{[T_2^v(t)]^2+(\Delta xt)^2\}^{\frac{D+1}{2}}} \tag{1}$$

Applying Tsallis machine the Generalized visiting distribution is:

$$g_{q_v}(\Delta xt) = c \frac{[T_{q_v}^v(t)]^d}{\left\{[T_{q_v}^v(t)]^e+(q_v-1)b(\Delta xt)^2\right\}^{\left(\frac{a}{(q_v-1)}\right)}} \tag{2}$$

being *a*, *b*, *c*, *d* and *e* parameters depending on *D* and *qV* where $d = e^{\left(\frac{2a-D(q_v-1)}{2(q_v-1)}\right)}$ ($\forall$ $q_v, \forall D$). After a set of simplifications results $d = \left(\frac{1}{(q_v-1)}\right)$ ($\forall$ $q_v, \forall D$) and equation 2 is:

$$g_{q_v}(\Delta xt) = \left(\frac{q_v-1}{\pi}\right)^{\frac{D}{2}} \frac{\Gamma\left(\frac{a}{(q_v-1)}\right)}{\Gamma\left(\frac{a}{(q_v-1)}-\frac{D}{2}\right)} \frac{[T_{q_v}^v(t)]^{-\left(\frac{D}{2a-D(q_v-1)}\right)}}{\left\{1+(q_v-1)\frac{\Delta xt^2}{[T_{q_v}^v(t)]^{\frac{2}{2a-D(q_v-1)}}}\right\}^{\left(\frac{a}{(q_v-1)}\right)}} \tag{3}$$

This expression could be more simplified considering an linear interpolation of qV obtaining $a = 1 + \left(\frac{D-1}{2}\right)(q_v-1)$ $(\forall\, q_v, \forall\, D)$ thus:

$$g_{q_v}(\Delta xt) = \left(\frac{q_v-1}{\pi}\right)^{\frac{D}{2}} \left[\frac{\Gamma\left(\frac{1}{(q_v-1)}+\frac{D-1}{(2)}\right)}{\Gamma\left(\frac{1}{(q_v-1)}-\frac{1}{2}\right)}\right]\left[\frac{[T_{q_v}^v(t)]^{-\left(\frac{D}{(3-q_v)}\right)}}{\left\{1+(q_v-1)\frac{\Delta xt^2}{[T_{q_v}^v(t)]^{\frac{2}{3-q_v}}}\right\}^{\left(\frac{1}{(q_v-1)}+\frac{D-1}{2}\right)}}\right] (\forall\, q_v, \forall\, D) \tag{4}$$

Additionally, it was proposed to generate a random vector $\Delta x = g^{-1}(\omega)$ and apply numerical integration to visiting distribution $g_{q_v}(x)$ for *D=1* [30], obtaining:

$$g_{q_v}(x) = \left(\frac{q_v-1}{\pi}\right)^{1/2} \frac{\Gamma\left(\frac{1}{(q_v-1)}\right)}{\Gamma\left(\frac{1}{(q_v-1)}-\frac{1}{2}\right)} \frac{[T_{q_v}^v(t)]^{-\left(\frac{1}{(3-q_v)}\right)}}{\left\{1+(q_v-1)\frac{x^2}{[T_{q_v}^v(t)]^{\frac{2}{3-q_v}}}\right\}^{\left(\frac{1}{(q_v-1)}-\frac{1}{2}\right)}} \tag{5}$$

being ω a random vector within the range *[0 1]* obtained from equiprobability distribution and g^{-1} is the inverse of integral of $g_{q_v}(x)$, therefore, $g^{-1}(\omega) = inverse\left(\int_{-\infty}^{x} g_{q_v}(x)\,dx\right) = inverse(\omega)$ and:

$$g^{-1}(\omega) = inverse\left\{\int_{-\infty}^{x} \left(\frac{q_v-1}{\pi}\right)^{1/2} \frac{\Gamma\left(\frac{1}{(q_v-1)}\right)}{\Gamma\left(\frac{1}{(q_v-1)}-\frac{1}{2}\right)} \frac{[T_{q_v}^v(t)]^{-\left(\frac{1}{(3-q_v)}\right)}}{\left\{1+(q_v-1)\frac{x^2}{[T_{q_v}^v(t)]^{\frac{2}{3-q_v}}}\right\}^{\left(\frac{1}{(q_v-1)}-\frac{1}{2}\right)}}\,dx\right\} \tag{6}$$

In order to solution of Δx, function integral was substituted by a polynomial series and the inverse truncated at order 17. In that way, $\Delta(x) = g^{-1}(\omega) = inverse\left(\int_{-\infty}^{x} g_{q_v}(x)\,dx\right) = inverse(\omega)$ and ω :

$$\omega = \omega(x) = \left(\frac{q_v-1}{\pi}\right)^{1/2} \frac{\Gamma\left(\frac{1-\frac{1}{2}(q_v-1)}{(q_v-1)}\right)}{\Gamma\left(\frac{1}{(q_v-1)}-\frac{1}{2}\right)} \int_{-\infty}^{x} \frac{a}{(1+bx^2)^c}\,dx \tag{7}$$

where: $a = [T_{q_v}^v(t)]^{-\left(\frac{1}{(3-q_v)}\right)}$; $b = \frac{(q_v-1)}{[T_{q_v}^v(t)]^{\frac{2}{3-q_v}}}$; $c = \frac{1}{(q_v-1)} - \frac{1}{2}$.

Using power law:

$$\omega = \frac{1}{2} + ax - \frac{1}{3}abcx^3 + \frac{1}{5}\left(\frac{1}{2}ac^2b^2 + \frac{1}{2}acb^2\right)x^5 + \cdots$$
$$\omega(x) = \omega_0 + A_1 x + A_2 x^3 + A_5 x^5 + \cdots$$
$$\omega(x) = \omega_0 + \sum_{n=1}^{\infty} A_n(x-x_0)^n \tag{8}$$

Operation on inverse function $g^{-1}=x=x(\omega)$ for *x(ω)-x=0* and equation 8, it is deduced that inverse function could be expressed in power series $x(\omega) = x_0 + \sum_{n=1}^{\infty} B_n(\omega - \omega_0)^n$. In that way, B_n coefficients are expressed as:

$$B_n = \frac{1}{nA_1^n} \sum_{\alpha,\beta,\gamma,\dots} (-1)^{\alpha+\beta+\gamma+\cdots} \frac{(n)(n+1)\dots(n-1+\alpha+\beta+\gamma+\cdots)}{\alpha!\beta!\gamma!\dots} \left(\frac{A_2}{A_1}\right)^{\alpha} \left(\frac{A_3}{A_1}\right)^{\beta} \tag{9}$$

where first coefficients of B_n are expressed as:

$$B_1 = \frac{1}{A_1}; B_2 = -\frac{A_2}{A_1^3}; B_3 = \frac{1}{3A_1^3}\left[\frac{(3)(4)}{2!}\left(\frac{A_2}{A_1}\right)^2 - \frac{(3)}{1!}\left(\frac{A_3}{A_1}\right)\right]; B_4 = \frac{1}{4A_1^4}\left[-\frac{(4)(5)(6)}{3!}\left(\frac{A_2}{A_1}\right)^3 + \right.$$

$$\left.\frac{(4)(5)}{2!1!}\left(\frac{A_2}{A_1}\right)\left(\frac{A_3}{A_1}\right) - \frac{(4)}{1!}\left(\frac{A_4}{A_1}\right)\right]$$

Therefore, those methods dispose of the original proposed Lévy flight distribution as visiting distribution [25] [30]. Four steps were established to minimize an objective function *E(x)* using GSA algorithm:

1) Fix *qV* over time *t=1* using random value of *x1* and ponderable highly value of *Tqv*(1) obtaining *E(x1)* and beginning quenching process as per equation 10:

$$T_{q_v}^v(t) = T_{q_v}(1)\frac{2^{q_v-1}-1}{(1+t)^{q_v-1}-1} \tag{10}$$

2) Randomly generate *x(t+1)* from *x(t)* using visiting distribution $g_{q_v}(\Delta xt)$ according to equation 11 determining jump size of $\Delta(xt)$ and defining isotropic direction, therefore, assuring the swing of search of the algorithm through the whole hypercube. Being $\Delta(xt) = g^{-1}(\omega)$ we obtain:

$$x(t+1) = x(t) + g^{-1}(\omega) \tag{11}$$

3) Determine *E(x(t+1))*:

    a) If *E(x(t+1))<E(xt)* substitute *xₜ* by *x(t+1)*;

    b) If *E(x(t+l))≥E(xt)* then a random value *r* within the range of *[0, 1]* should be used. If the value of *r* is greater than generalized acceptation probability *PqA* as formulated in equation 12 with $T_{qA}^A(t) = T_{q_v}^v(t)$ the value of *xₜ* should be retained, otherwise, substitute *xₜ* by *x(t+1)*.

$$P_{q_A}(xt \dashrightarrow x(t+1)) =$$

$$\begin{cases} 1 \; se \; E(x(t+1)) \le E(xt) \\\\ \dfrac{1}{\{1+[1+(q_A-1)(E(x(t+1))-E(x(t)))/T_1^A(t)]\}^{\left(\frac{1}{(q_A-1)}\right)}} se \; E(x(t+1)) > E(xt) \end{cases} \tag{12}$$

where *A* and *qA* match with Boltzmann machine parameters with value *1*. Likewise, *V* and *qV* match with Cauchy machine parameters with value *2*.

4) Calculate the new value of $T_{q_v}^v(t)$ using equation 11, so go back to step *2* and continue till to reach *E(xₜ)* minimum within the established tolerance.

2.1.3 A novel Hybrid Generalized Simulated Annealing Algorithm, GSA-HYBRID

In order to avoid GSA "leap" when nearly optimal value is reached, a novel Hybrid Generalized Simulated Annealing Algorithm is proposed. This novel technique was inspired from gradient convergence technique [32]. Hypotheses of this novel technique established that the increment of probabilistic space variable from equation 7 (random vector $\Delta x = g^{-1}(\omega)$) was transformed into a deterministic variable as the fitness objective function value is nearly to minimum. For this purpose, a boolean was determined to continue the step 2 from equation 11, however, using the deterministic vector Δx till the minimum global is reached. This Δx assumes conveniently the tolerance value imposed to fitness parameters values. On the other hand, Δx adopts increment or decrement value depending on whether the nearly objective function value is before or after the global minimum value, respectively. This criteria continue the same strategy imposed in step 2 equation 11 of GSA, however considering the deterministic increment Δx. As the global minimum value is achieved the boolean is finalized turning the deterministic increment Δx to its natural probabilistic origin.

Following the methodology, the case of study of infiltration is set forth.

2.2 Case of study of infiltration

Infiltration was represented by an experiment in the laboratory as shown in figure 1 [7] [40]. The continuous water flux on experiment simulates rainfall, thus, the water table grows because water infiltrates through unsaturated soil. The experiment was divided symmetrically with all-known constraints. Thus, upper boundaries are known flux, potential is known when the infiltration reaches the water table, all-known flux at the sides and the bottom of the domain. For more details, reference is given [7]. Conditions of the experiment are homogeneous soil and bidirectional flux because of the minimum thickness between the crosswise direction plates of the experiment.
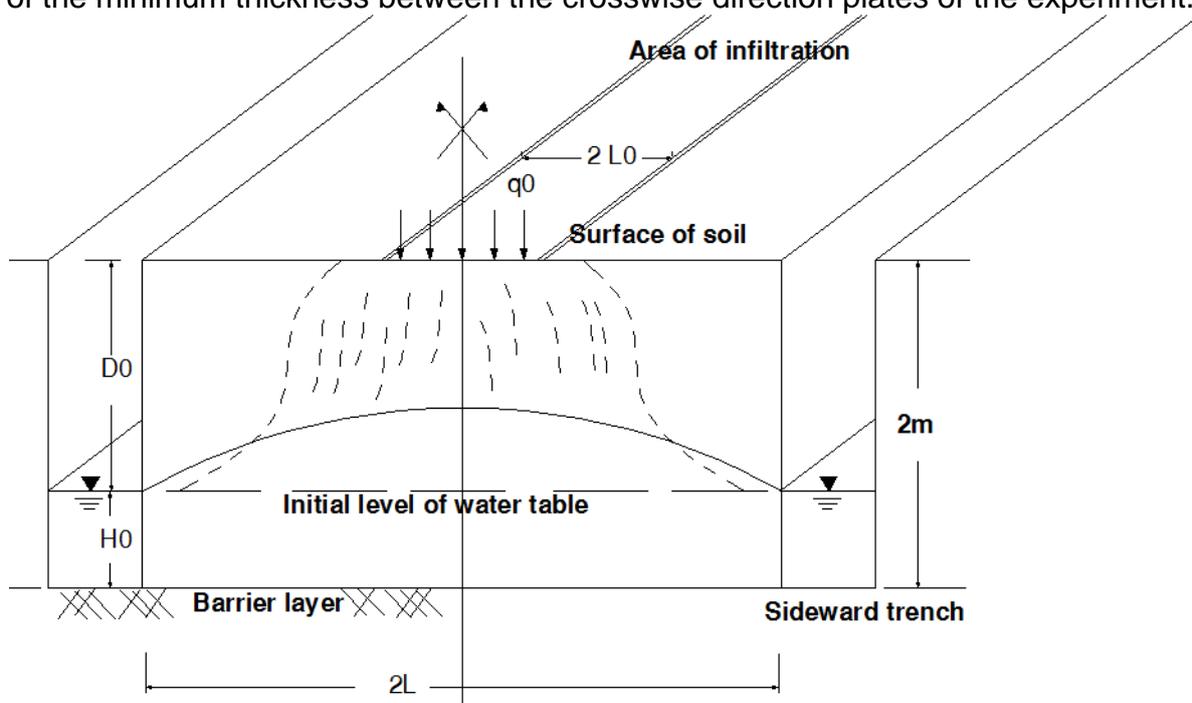
Fig. 1. Design of the laboratory experiment, modified from [7].

Following the methodology figure 2 shows input of ordered pairs of matric potential and volumetric content obtained from the experiment of Vauclin [7]. Stochastic nature of the experiment is set forth at the figure 2 due to different values of volumetric content corresponding to the same value of matric potential. No matter how carefully the experiment, small perturbations emerged from the complex system. As shown in figure 2, upper and bottom limit of retention curves was implemented in order to establish a search field for optimization algorithms. Thus, simulated parameters obtained from calibration of the model of infiltration are verified through the retention curve response. Range of physical parameters sets up the form of those limit retention curves. Differently from mathematical functions where no setup searching boundaries, natural infiltration modeling conditions demand those searching limit retention curves.
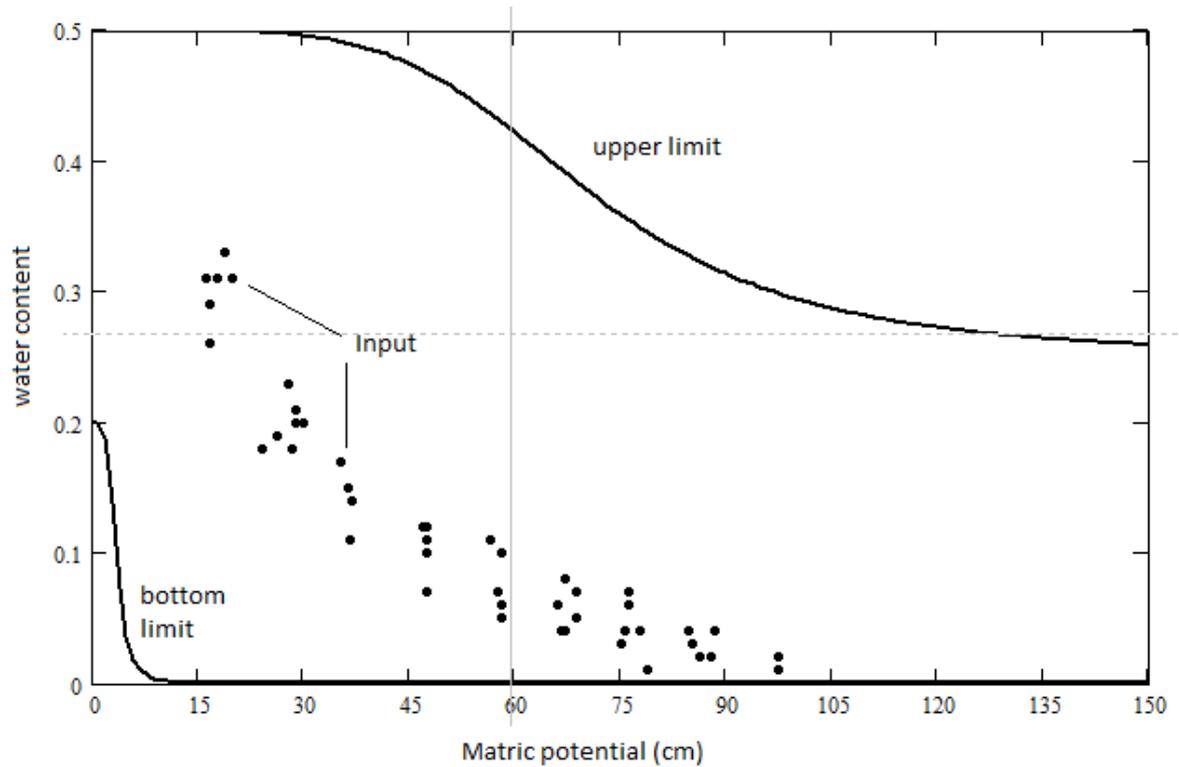
Fig. 2. Upper and bottom limit search domain, input from experiment is set forth [7].

Parameters of the MVG [14] were implemented as parameters of the global model as set forth in equations 13 and 14:

$$\frac{\theta_i^{\,j} - \theta_{res}}{\theta_{sat} - \theta_{res}} = \left[\frac{1}{1 + (\alpha |\psi_i^{\,j}|)^n} \right]^m \tag{13}$$

where: i indicates space, j indicates time, $\theta_i^{\,j}$ is the water content in space i and time j; θ_{sat} represents the saturated water content, θ_{res} is the residual water content, $\psi_i^{\,j}$ is the matric potential (L); α is the MVG model coefficient (L^{-1}); n is the non-dimensional coefficient; $m=(n-1)/n$,

$$K_i^{\,j} = K_{sat} \left(\frac{\theta_i^{\,j} - \theta_{res}}{\theta_{sat} - \theta_{res}} \right)^{1/2} \left\{ 1 - \left[1 - \left(\frac{\theta_i^{\,j} - \theta_{res}}{\theta_{sat} - \theta_{res}} \right)^{1/m} \right]^m \right\}^2 \tag{14}$$

where: $K_i^{\,j}$ is the hydraulic conductivity in space i and time j being the same value for x, y, z due to isotropic soil characteristic (L/T); K_{sat} is the saturated hydraulic conductivity for x, y, z (L/T); remaining parameters were defined.

Table 1 represents parameter value ranges from retention curves called "upper limit" and "bottom limit".

Table 1. Van Genuchten modeling parameters value range [14]

Parameters	n	α	K_{sat} (cm/h)	θ_{sat}	θ_{res}
Highest value	15.00	0.5000	350.00	0.50	0.50
Lowest value	1.01	0.0001	0.00	0.00	0.00

Figure 3 sets forth eleven control points of water table level and hypercube discretized in triangular finite elements. Two control points (**+**) were gauged at two hours, three control points (**◆**) were sized at three hours, four control points (**■**) were measured at four hours, six control points (**●**) was measured at six hours [7, 4, 41].
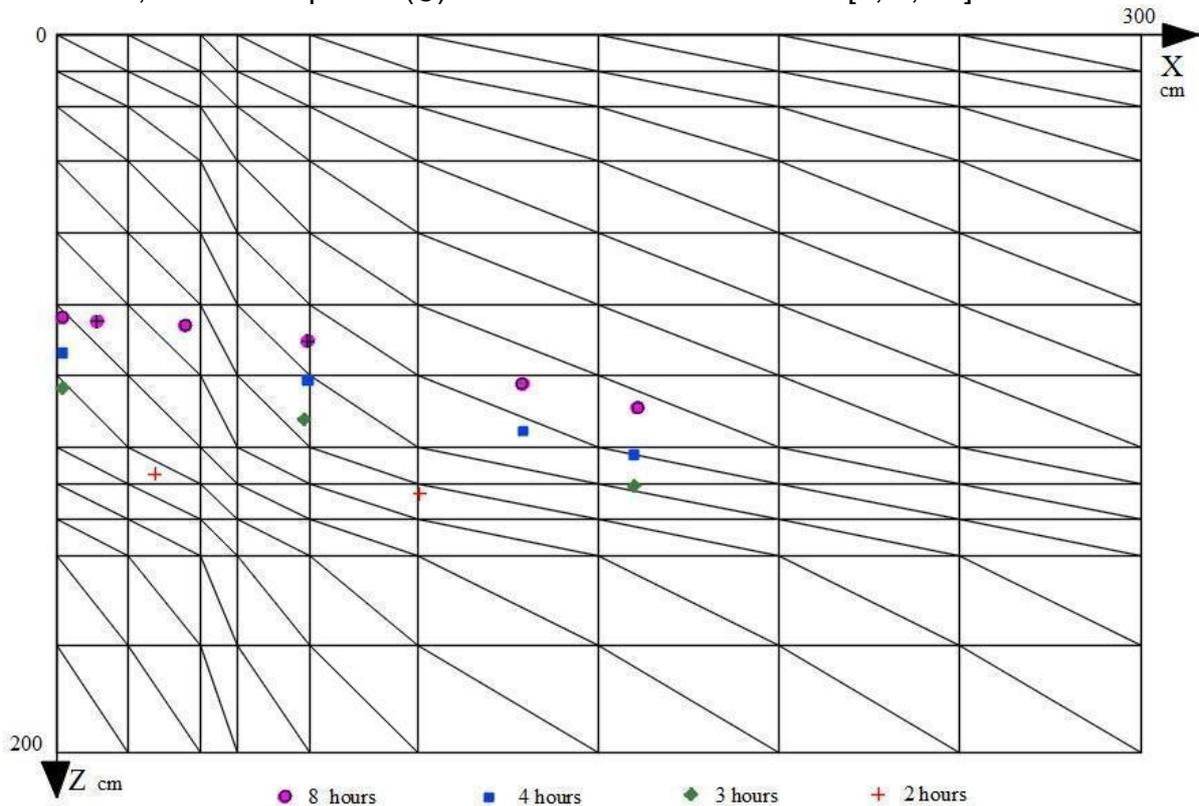

Fig. 3. Net imposed over physical experiment domain [7], control points of water table level are set forth.

2.3 Fitness of Goodness, Objective Functions responses

As aforementioned fitness goodness depends on an objective function (OF). Difference between input and output at control points minimize an OF as per equation 15:

$$MIN\ FO = \sum_{i=1}^{n}(|P_{i_{Observed}} - P_{i_{Simulated}}|)^2 \tag{15}$$

where: $Pi_{observed}$ and $Pi_{simulated}$ are the matric potential inputs at control point i over time and space; n is the total number of control points, in this case n=15; $\sum_{i=1}^{n}(|P_{i_{Observed}} - P_{i_{Simulated}}|)^2$ is the result of a quadratic sum of difference between $Pi_{observed}$ and $Pi_{simulated}$ all over the control points.

2.4 Simulation of complex system of infiltration

Complex system simulation of infiltration is based in Richards equation [8] expressed as:

$$\frac{d}{dx}\left[K_x(\Psi)\frac{d\Psi}{dx}\right] + \frac{d}{dz}\left[K_z(\Psi)\left(\frac{d\Psi}{dz}+1\right)\right] = \frac{d\theta}{dt} \tag{16}$$

where Ψ is the matric potential [L]; z is the downward positive vertical direction [L]; $\frac{d\theta}{dt}$ is the vector rate of θ divided by time [T^{-1}]; $\frac{d\Psi}{dx}, \frac{d\Psi}{dz}$ are the vector composed of rate of

Ψ divided by x and z directions, respectively [LL^{-1}]; $\frac{d}{dx}\left[K_x(\Psi)\frac{d\Psi}{dx}\right]$ is the vector composed of rate of the product between x-direction hydraulic conductivity variable in function of matric potential by $\frac{d\Psi}{dx}$ [T^{-1}]; $\frac{d}{dz}\left[K_z(\Psi)\left(\frac{d\Psi}{dz}+1\right)\right]$ is the vector rate of the product between z-direction hydraulic conductivity variable in function of matric potential by the sum between $\frac{d\Psi}{dx}$ and 1 value, due to the gravity effect [T^{-1}].

Equation 16 was numerically resolved using different techniques. Afterwards, Finite elements method (FEM) and Finite difference method (FDM) were applied to simulate a complex system of infiltration over space and time, respectively. Matric potential values (ψ) were determined using FEM at each finite element. For this purpose, interpolation functions were utilized, subjected to constraints of physical phenomenon. Meanwhile, residual values are generated from the difference among matric potential values determined from finite elements that converge at each node of the mesh and the exact solution. Those residual values are redistributed all along the domain using the residual pondered method which in turn utilizes pondered functions. Galerkin method was selected from several residual pondered methods due to the advantage of pondered functions and interpolation functions are the same. Integration by parts was utilized to solve pondered residuals. Afterwards, equation that governs flux of water in unsaturated soil is solved through assemble of matrices at each finite element as set forth in equation 17:

$$\underline{ConductivityMatrix}|\psi| + \underline{RetentionMatrix}\left|\frac{d\psi}{dt}\right| = \underline{NodeFlow} - \underline{GravityFlow} \quad (17)$$

where $\underline{ConductivityMatrix}$ is the matrix of flux referring to water conductivity in unsaturated soil; $\underline{RetentionMatrix}$ is the matrix linked to water retention capacity; $\underline{NodeFlow}$ is the matrix flow through contour domain simulated on nodes of finite element from that contour domain; $|\Psi|$ is the vector with Ψ values at all nodes from finite elements; $\left|\frac{d\Psi}{dt}\right|$ is the vector rate of Ψ divided by time at all nodes from finite elements. Afterwards, Picard iteration method is applied to solve equation 17. This method implements time steps and diminishes time till equation 17 is solved, subsequently, more time steps are employed to reach the total time of the physical phenomenon [4, 41–43].

As a follow-up to find parameters of the model, an automatic calibration method is described.

2.5 Scheme of calibration model process

Figure 4 sets forth the scheme of automatic calibration model processes that tackle the study of infiltration phenomena. As per this procedure, the parameter vector is established randomly. In this case, there are five parameters (n, α, K_{sat}, θ_{sat}, θ_{res}) from equations 14 and 15 belonging to the MVG model. Afterwards, this parameter vector is underway to equations 16 and 17 solving the equation that governs the flux or water in unsaturated soil. After that, output and input values are submitted to equation 15 fitting the objective function. Subsequently, if objective function values called "goodness of fit" reaches tolerance criteria established then a novel arbitrarily parameter input vector is created by the Optimization algorithm. Thus, a new cycle is initiated till to achieve tolerance criteria and subsequent appraisal of results.
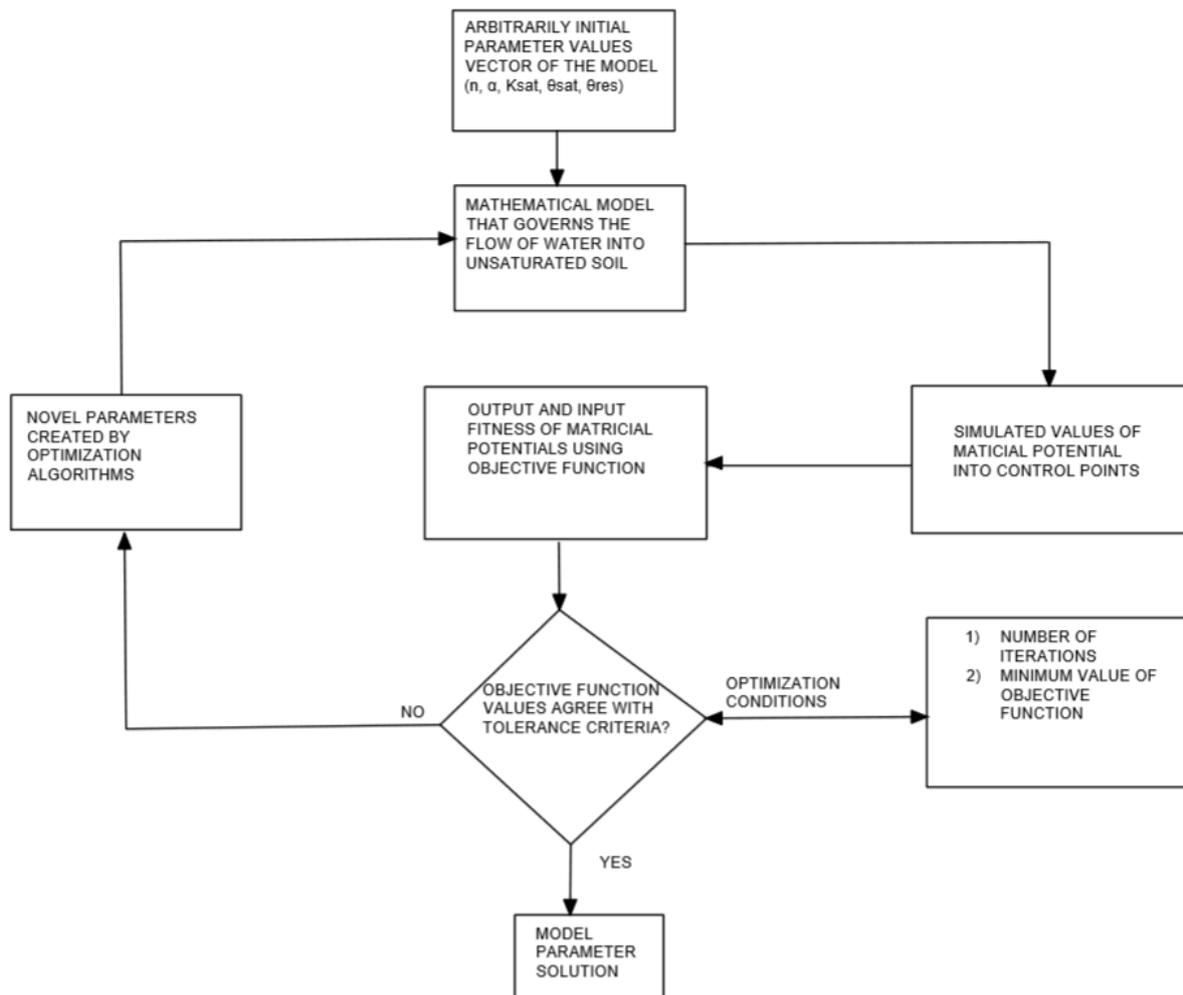
Fig. 4. Scheme of automatic calibration model using optimization algorithm.

3. Results and discussion

Results from application of optimization algorithms over case study are discussed. Case studies approached are first a mathematical function and subsequently the infiltration case study.

3.1 Test of optimization algorithm applied to mathematical function

Figure 5 sets forth the test mathematical function called Ackley function that shows several local optimums and one global optimum. Equation 18 is the mathematical expression of the function:

$$f(x) = -a \exp\left(-b\sqrt{\frac{1}{d}\sum_{i=1}^{d} x_i^2}\right) - \exp\left(\frac{1}{d}\sum_{i=1}^{d}\cos(cx_i)\right) + a + \exp(1) \qquad (18)$$

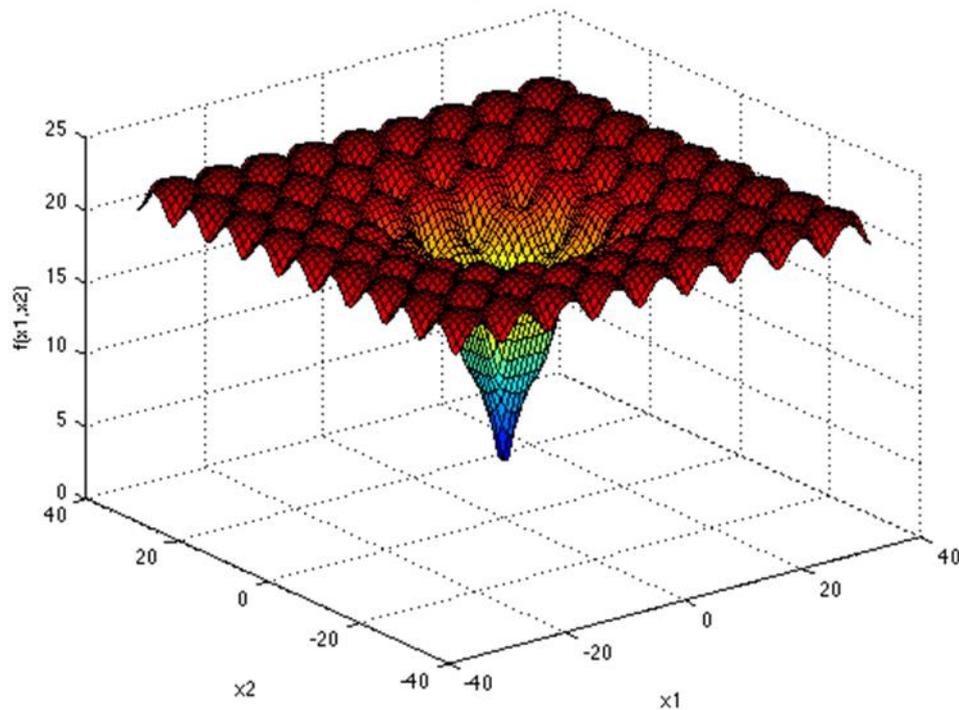where recommended parameter values are a=20, b=0,2, c = 2π e d=2 [44].

Fig. 5. Ackley function showing several local minimums and one global minimum [44].

A Personal Computer (PC) Intel® Core™ i7 was used for the proposed mathematical modeling process. Figure 6 shows that Genetic Algorithms - GAs reaches the global optimum over 16 seconds while GSA (Generalized Simulated Annealing) achieves the global optimum almost instantly and definitely at almost 2 seconds.

Furthermore, Figure 6 shows that whereas the GA carries out a continuing search for the optimum global, GSA performs a "leap" using the criteria of Metropolis algorithm and doing a broader search.
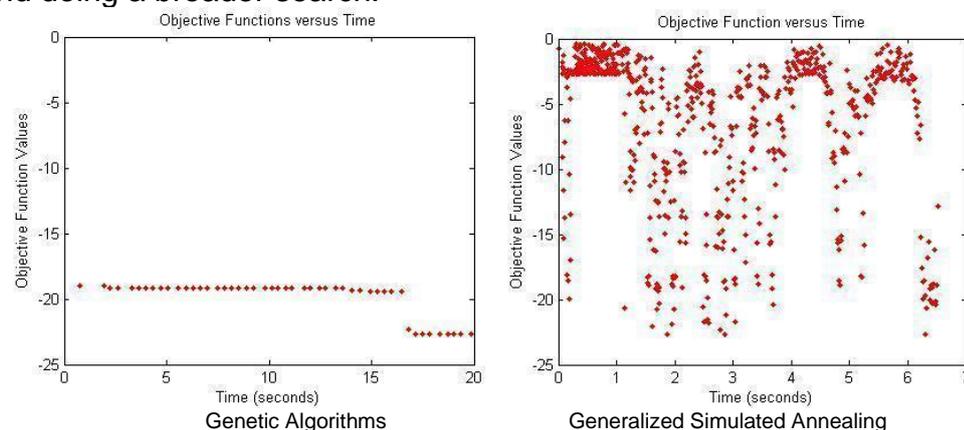

Fig. 6. Comparison of results between Genetic Algorithms - GAs and Generalized Simulated Annealing - GSA for fitness of ACKLEY mathematical function.

In this work, as aforementioned in section 2.1.3, the effect of reaching an instantaneously nearly GSA result and then "leap" (Figure 6) is treated using convergence gradient method to obtain the minimum value without "leap" when fitness value is proximate to minimum that we called GSA-hybrid.

GSA-hybrid technique results are shown in Figure 7. Fitness of Objective function versus time and space are presented, respectively. As aforementioned, GSA-

hybrid criteria do not allow GSA "leaps" from the nearly global minimum forcing GSA to reach the optimal value. In that case, achieving optimal results the GSA is accepted to continue its "leap" through the extensive domain. Figure 7a shows the approximately first result of GSA converging to the lowest value. Gaps of figure 7a represent the "leaps" of GSA out of the range of figure, however, as soon as it becomes near the region of minimum, once more GSA-hybrid forces GSA to achieve the minimum. The first optimum value was reached at 0.12 seconds as shown in figure 7a, however that minimum is achieved frequently. Figure 7b set forth the advance of convergence through space. GSA-hybrid criteria hold the variation of mathematical functions on the way toward the optimum.

Figure 7b establishes the robustness of GSA-hybrid. For instance, Genetic Algorithms demonstrate robustness "crawling" step by step in domain to reach the minimum global without PC memory problem or stopping abruptly the code. The same way, Figure 7b set forth GSA-hybrid robustness achieving the minimum global without any abrupt interruption. On the contrary, GSA-hybrid arrives at minimum global lots of times as shown at figure 7a.
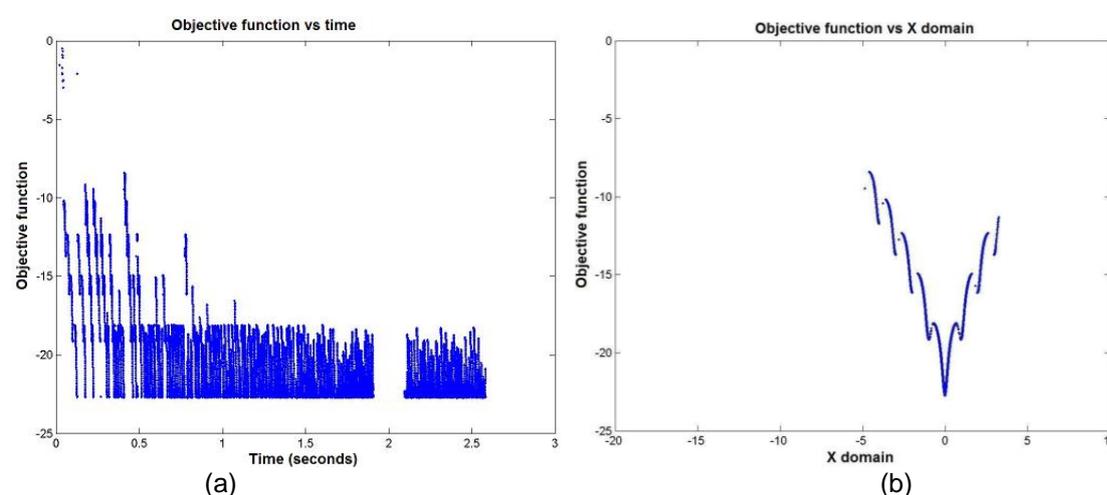

Fig. 7. Results of GSA-hybrid for ACKLEY mathematical function. (7a) shows Objective functions values versus time (seconds) and (7b) identifies Objective function values versus space.

3.2 Optimization algorithm applied to case study of infiltration

A personal computer Intel® Core™ i7 was used as a computational power to simulate infiltration phenomenon. Figure 8 set forth the results of objective function fitness versus time using both Genetic Algorithms and Generalized Simulated Annealing. That figure 8 shows the results from GA using the personal computer and MATLAB code obtaining a fitness value of 2658 in two hours and half. Nevertheless, it is important to indicate that in the literature [40] the results from GA using a cluster and FORTRAN code obtained a fitness value of 400 in seven days for the same experiment. As such, in order to compare optimization algorithms, the cluster results in literature is enough.

Back to figure 8, output fitness values versus time is set forth using the GSA algorithm. GSA obtains several "penalized values" of 10000. GSA reaches the minimum fitness value of 40 in twenty minutes. This result is appropriate considering that zero result is not possible due to imperfections of a complex system of infiltration.

This feasible result of GSA derives from the searching power, such as, the visiting distribution methodology and generalized acceptance probability. Therefore,

GSA is more efficient than Genetic Algorithms with its operators of mutation, creep, crossover, and so on. Furthermore, GSA could improve its fitness results by handling the number of iteration cycles, initial temperature value and so on.

As set forth in figure 8 GSA practically reaches the minimum value at approximately 50 seconds then "leap". In order to avoid GSA "leap" as near to the optimal result it is applied the conjugate convergence gradient method called GSA-hybrid.

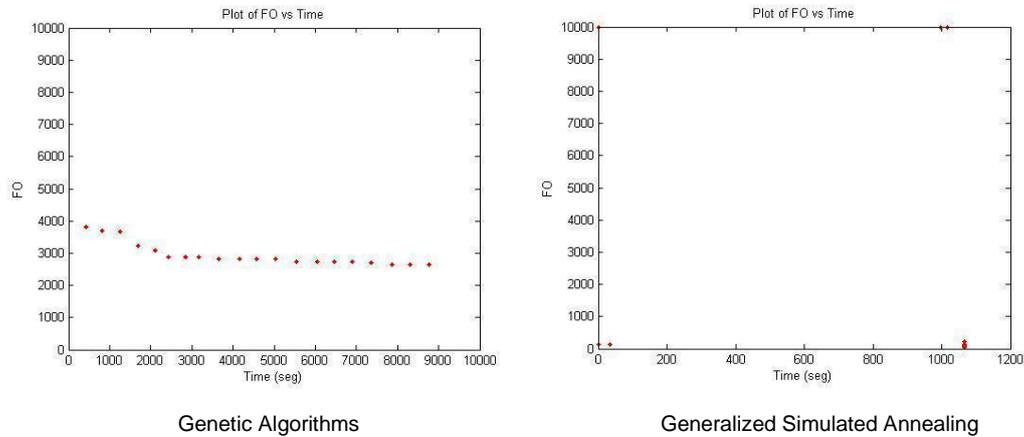Genetic Algorithms   Generalized Simulated Annealing

Fig. 8. Comparison of results between Genetic Algorithms and Generalized Simulated Annealing applied to case study. Observed that GSA almost reaches the minimum value at 50 seconds.

Figure 9 sets forth objective function GSA-hybrid minimum value (33.5) less than GSA value (40) on figure 8. Again, zero value as optimum is not reached due to imperfections in the infiltration complex system model. Whatever, GSA-hybrid showed better performance obtaining the minimum value at seven minutes. As shown in figure 9, GSA-hybrid do not allow a response near to optimum to "jump" forcing GSA to achieve the minimum. After that, the GSA is unleashed to continue its "jump".
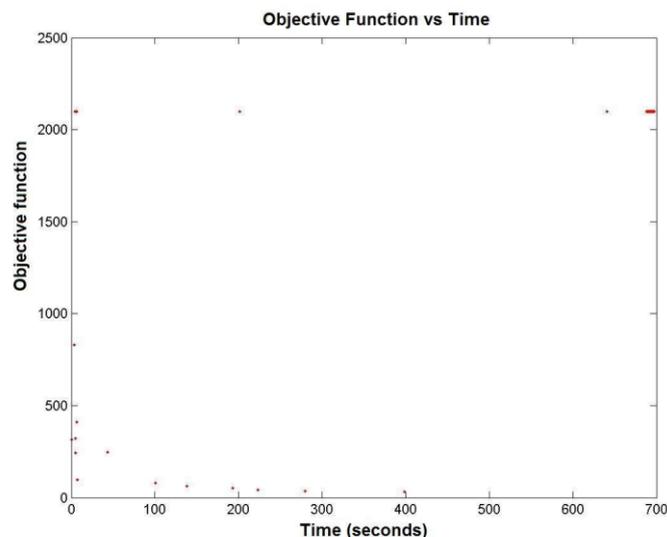

Fig. 9. Convergence of infiltration phenomenon model using GSA-hybrid algorithm. Consider that a value near to optimal is "trapped" to descend to optimum result.

Table 1 shows computational time covered by optimization algorithms performing simulation of infiltration. This table utilizes the best computational time

covered by CLUSTER (168 hours) using Genetic Algorithms [40]. On the other hand, as the case study runs in Personal Computer, Genetic Algorithms use 1000 generations and people of five individuals (Genetic Algorithms terms) whereas Generalized Simulated Annealing (GSA) utilizes 200 cycles demonstrating that GSA was extremely fast.

Nevertheless, GSA "ignores" nearly optimum values. In that case, GSA-hybrid force GSA reaches that optimum before GSA continues its "jumping". Table 1 sets forth the time used by GSA-hybrid performing fastest.

Table 1. Comparison of computational time of optimization algorithms

	Optimization algorithms		
Application	GAs	GSA	GSA-hybrid
Ackley mathematical function	16 seconds	2 seconds	0.12 seconds
Complex system of infiltration	168 hours (CLUSTER)	20 minutes	7 minutes

Table 2 sets forth a comparison of the five-parameter van Genuchten model (n, α, K_{sat}, θ_{sat}, θ_{res}) determined by Genetic Algorithms and Generalized Simulated Annealing [14]. Table 2 shows the experimental parameters (K_{sat}, θ_{sat}, θ_{res}) determined by Vauclin et al. [7]. It is observed from table 2 that the resulting values of the empirical parameters (n and α) of the model obtained by both algorithms present similar values. The value of the experimental hydraulic conductivity parameter (K_{sat}) differs from the simulated result of the Genetic Algorithms in the order of 3 *cm/h* and the GSA algorithm in the order of 5 *cm/h*. In general, simulated results from GA and GSA of saturated water content θ_{sat} (*cm³/cm³*) and residual water content θ_{res} (*cm³/cm³*) are close to experimental values. Sensitivity of parameters simulated values cause significant differences in objective function values consequently demanding higher computational cost. Trying to find exactly experimental parameters values is not possible because infiltration is a complex system with inherent perturbations. Likewise, anchoring a believed real parameter value to search others parameters is not appropriate because of the same reason of imperfections in a complex system and the sensibility of its parameters [4]. Nevertheless, GSA-hybrid overcomes those difficulties performing reasonably and fastest. GSA-hybrid parameters resulted values are compared with parameters experimental values [7] and simulated parameters values obtained from GAs and GSA.

Table 2. Comparison of simulated parameter values obtained by optimization algorithms, also, experimental parameter values [7]

	n adimensional	α cm^{-1}	K_{sat} (cm/h)	θ_{sat} (cm³/cm³)	θ_{res} (cm³/cm³)
Experimental parameter input	----	----	35.0000	0.30	0.00
Genetic Algorithms - GAs	3.57	0.030	32.2200	0.310	0.020
Generalized Simulated Annealing - GSA	4.13	0.024	30.0819	0.298	0.010
GSA-hybrid	4.56	0.027	31.5123	0.254	0.006

Figure 10 sets forth characteristic curves using parameters from table 2. Those characteristic curves are not obtained in different and isolated experiments, on the contrary, this event is just a one of the several constatations of the modeling automatic calibration of infiltration. In that figure 10, the solid line represents the characteristic

curve fitness called "Vauclin curve" derived from the least square method applied to input ordered pairs (Ψ, θ). The point line is the characteristic curve called "GA curve" based on parameters determined by Genetic Algorithms. The major dashed line represents the characteristic curve called "GSA curve" using parameters obtained by Generalized Simulated Annealing and, at last, the minor dashed line indicates the characteristic curve called "GSA-hybrid curve". All of those optimization algorithms obtained the reverted "S" approximated to the characteristic curve obtained by the author of the experiment [7]. Nevertheless, GA curve sets forth deficiency at the plateau and the tail, whereas GSA curve performs reasonably. Meanwhile, GSA-hybrid fitness shows the plateau with the minor value compared with the others algorithms and the experimental value, however, the tail is closer to the experimental value.
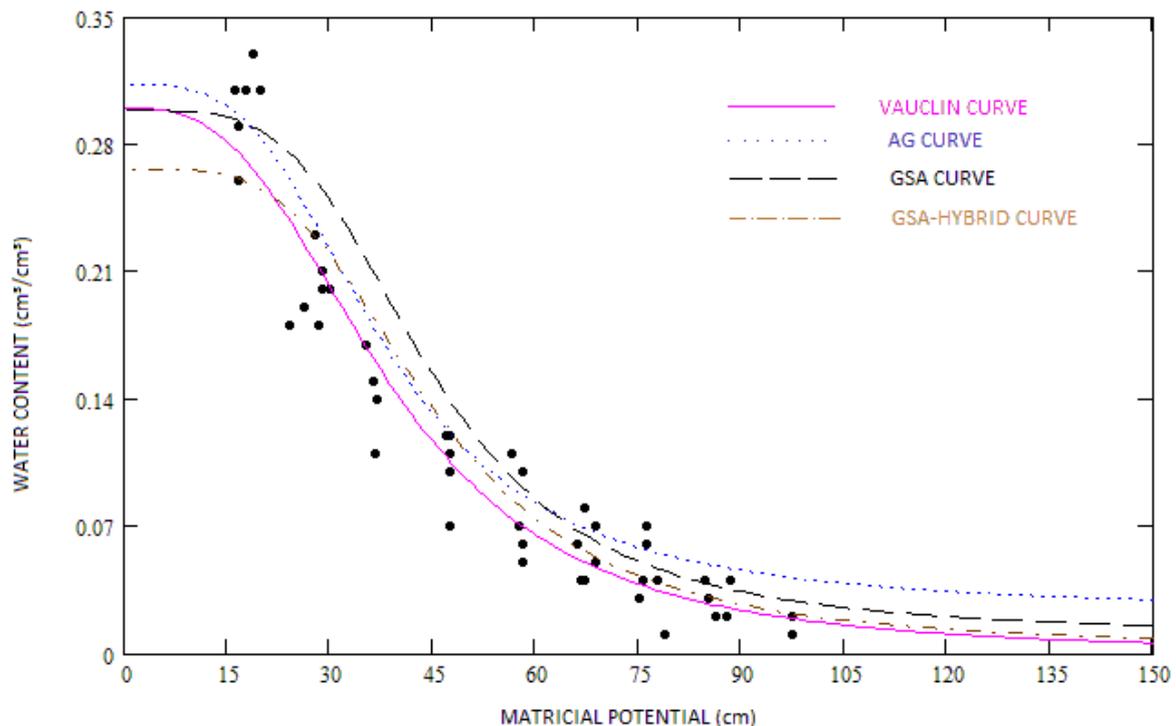

Fig.10. Comparison of retention curve from van Genuchten model [14], "GA Curve" obtained by Genetic Algorithms, "GSA Curve" obtained by Generalized Simulated Annealing and "GSA-hybrid curve". Additionally, it is shown the "Vauclin Curve" obtained by least quadratic method [7].

Figure 11 sets forth another validation of results. Water table levels over time are represented in that figure 11 corresponding to Vauclin fitness in dashed lines, Genetic Algorithms fitness is represented in solid lines, Generalized Simulated Annealing fitness is shown in lower dashed lines and GSA-hybrid algorithm fitness is set forth in diminished dashed lines. In this simulation figures 10 and 11 are joined in one event, differently from the original author's proposal where those figures were represented on isolated experiments [7, 40].
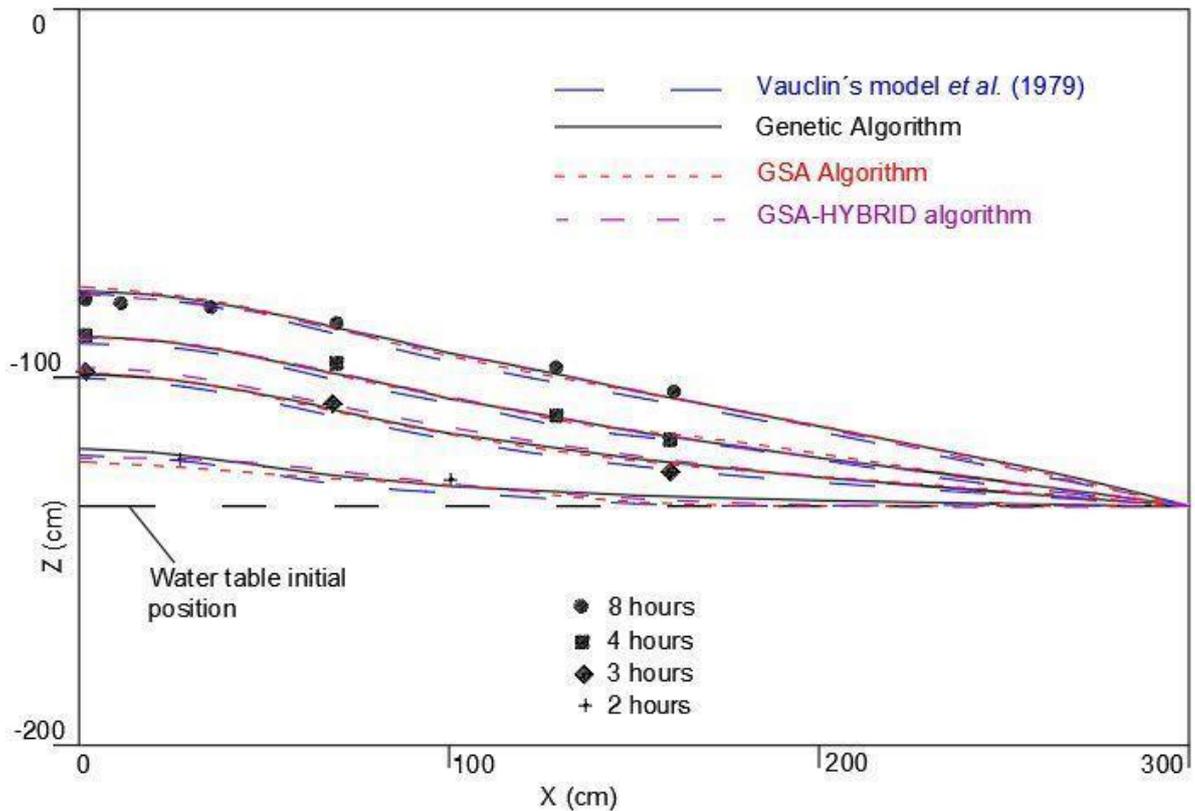
Fig.11. Control points of Vauclin´s experiment and water table levels in different times represented by: dashed lines obtained by Vauclin model, GSA model and GSA-hybrid model. Solid lines were obtained by GA technique. Scale in centimeters.

4. Conclusions

Simulation of a complex system of infiltration confined at a laboratory experiment highlighted the importance of this work.

The objectives of this paper were achieved due to correct function of items as: discretization of physical phenomena on time and space, equation that governs flux of water in unsaturated soil, modeling of retention curve, inverse model, objective function and implementation of optimization algorithms.

Established constraints hypothesis applicable to the physical phenomenon modeling performed suitable achieving a dynamically simulated water table.

High sensibility parameters of the model searched by optimization algorithms represented a hard task, however those algorithms were capable of circumventing that difficulty.

The crucial hypothesis applied to GSA-HYBRID in relation to changing the probabilistic nature of advance in the domain to a deterministic advance carried out successfully.

The diminution of possible perturbations from experiment guided the selection of this case study. Nevertheless, those noises do not disappear at all due to the inherent stochastic complex system of infiltration.

Method Finite Element applied to discretize the domain and Method of Difference Finite used to discretize the time of experiment performed appropriately. The time consumed by both discretizations were reasonable as per the phenomenon model.

The formulation of the Objective function based on minimization of the sum of quadratic differences between observed and simulated matric potential was suitable. However, the ideal minimization was not achieved due to the stochastic nature of physical phenomena.

The program's tolerance condition imposed on the mathematical model was appropriate due to the good performance of penalizing results once this tolerance was reached. Likewise, the condition of the interruption program established by the total number of "generations" of Genetic Algorithms or total number of cycles of GSA and GSA-hybrid was achieved completely. Both conditions warranted the flux of the program till the final of the process.

References of literature utilized in this paper identify original authors of handle techniques. Additionally, those references established the state-of-art of those techniques leaving a way to contribute through this work to the real scene.

Results of Genetic Algorithms established a good benchmark to which GSA and GSA-HYBRID accomplished to overcome.

Tsallis' function probability as a GSA technique was completely verified, giving GSA the powerful tool of "jump" through the whole domain consuming less computational time. Furthermore, the GSA-HYBRID technique using the convergence gradient concept routed the nearest result of global minimum to the final global minimum. GSA-HYBRID impressively reduces the computational time using a personal computer configuring a strong reason to use this technique in future case studies.

Determination of initial values of parameters reducing the expensive experimental cost of collecting inputs from fields makes suitable the use of GSA-HYBRID.

Finally, GSA-HYBRID is easy to handle and be implemented in whatever code of a mathematical model.

CONFLICT OF INTERESTS

Authors declare no conflict of interests.

AUTHORS CONTRIBUTIONS

Thiago Barros Murari contributes to the structure of the article. Marcelo Moret is one of the collaborators to improve the technique of the GSA Algorithm.

References

1. Sihag, P.; Singh, B.; Vand, A.S.; Mehdipour, V. Modeling the infiltration process with soft computing techniques. *ISH Journal of Hydraulic Engineering* **2018**, *26*, 138-152, doi:10.1080/09715010.2018.1464408. [CrossRef]
2. Kumar, S.; Kaushal, D.R.; Gosain, A.K. Evaluation of evolutionary algorithms for the optimization of storm water drainage network for an urbanized area. *Acta Geophysica* **2019**, *67(1)*, 149–165, doi:10.1061/(ASCE)CP.1943-5487.0000157. [CrossRef]
3. Wang, K.; Yang, X.; Li, Y.; Liu, C.; Guo, X. An Application of Chaos Gray-Encoded Genetic Algorithm for Philip Infiltration Model. *Thermal Science* **2018**, *22(4)*, 1581-1588, doi:10.2298/TSCI1804581W. [CrossRef]
4. D'Aniello, A.; Cimorelli, Luigi; Cozzolino, L. The Influence of Soil Stochastic Heterogeneity and Facility Dimensions on Stormwater Infiltration Facilities Performance. *Water Resources Management ·***2019**, *33(7)*, 1-17, doi:10.1007/s11270-017-3674-0. [CrossRef]
5. Teixeira, C.F.A.; Moraes, S.O.; Simonete, M.A. Desempenho do Tensiômetro TDR e Sonda de Nêutrons na Determinação da Umidade e Condutividade Hidráulica do Solo. *Revista Brasileira de Ciências de Solo* **2006**, *29*, 161-168, doi:10.1590/S0100-06832005000200001. [CrossRef]
6. Gvirtzman, H.; Shalev, E.; Dahan, O.; Hatzor, Y. Large-scale infiltration experiments into unsaturated stratified loess sediments: Monitoring and modeling. *Journal of Hydrology* **2008**, *349*, 214–229, doi:10.1016/j.jhydrol.2007.11.002. [CrossRef]

7. Vauclin, M.; Khanji, D.; Vachaud, G. Experimental and numerical study of a transient, two-dimensional unsaturated-saturated water table recharge problem. *Water Resources Research* **1979**, *15(5)*, 1089-1101. doi: 10.1029/WR015i005p01089. [CrossRef]

8. Richards, L.A. Capillary Conduction of Liquids in Porous Mediums. *Physics* **1931**, *1(5)*, 318-333, doi:10.1063/1.1745010.

9. Wang, K.; Yang, X.; Li, Y.; Liu, C.; Guo, X. An Application of Chaos Gray-Encoded Genetic Algorithm for Philip Infiltration Model. *Thermal Science* **2018**, *22(4)*, 1581-1588, doi:10.2298/TSCI1804581W. [CrossRef]

10. Aguero-Martinez, D.S.; Murari, T.B.; Souza, F.B.O.; Moret, M.A. Calibração de Modelo de Fluxo Subsuperficial em Escala Menor Adotando os Algoritmos NSGA II, PADDS E MOPSO. *Revista Cereus* **2019**, 11(3), 190-211, doi:10.18605/2175-7275/cereus. [CrossRef]

11. De Carlo, L.; Berardi, M.; Vurro, M.; Caputo, M.C. Geophysical and hydrological data assimilation to monitor water content dynamics in the rocky unsaturated zone. *Environmental Monitoring and Assessment* **2018**, 190(310), doi:10.1007/s10661-018-6671-x. [CrossRef]

12. Jha, M.; Datta, B. Three-Dimensional Groundwater Contamination Source Identification Using Adaptive Simulated Annealing. *Journal of Hydrologic Engineering* **2013**, 18(3), doi:10.1061/(ASCE)HE.1943-5584.0000624. [CrossRef]

13. Gardner, W. R. Calculation of capillary conductivity from pressure plate outflow data. *Soil Science Society of America Journal* **1956**, 20(3), 317–320, doi:10.2136/sssaj1956.03615995002000030006x. [CrossRef]

14. Van Genuchten, M.Th. A closed-form equation for predicting the hydraulic conductivity on unsaturated soils. *Soil Science Society of America Journal* **1980**, 44, 892-898, doi:10.2136/sssaj1980.03615995004400050002x. [CrossRef]

15. Ramos, T. B.; Gonçalves, M. C.; Martins, J. C.; Pires, F. ; Pereira, L.S. Propriedades hidráulicas do solo para as diferentes classes texturais. *Revista de Ciências Agrárias* **2011,** 34(2), 252-264, doi:10.19084/rca.16023. [CrossRef]

16. Papafotiou, A.; Helmig, R.; Schaap, J.; Lehmann, P.; Kaestner, A.; Flühler, H.; Neuweiler, I.; Hassanein, R.; Ahrenholz, B.; Tölke, J.; Peters, A.; Durner, W. From the pore scale to the lab scale: 3-D lab experiment and numerical simulation of drainage in heterogeneous porous media. *Advances in Water Resources* **2008**, 31(9), 1253–1268, doi:10.1016/j.advwatres.2007.09.006. [CrossRef]

17. Philip, J.R. The theory of infiltration-3: moisture profiles and relation to experiment. *Soil Science, Baltimore* **1957a**, 84, 163-78, doi:10.1097/00010694-195708000-00008. [CrossRef]

18. Philip, J.R. The theory of infiltration: 4. Sorptivity and algebraic infiltration equations. *Soil Science, Baltimore* **1957b**, 84(3), 257-265, doi:10.1097/00010694-195709000-00010. [CrossRef]

19. Holland, J. H. *Adaptation in natural and artificial systems: an introductory analysis with applications to biology, control and artificial intelligence*. University of Michigan Press, Ann Arbor, Michigan, USA, 1975, ISBN 978-047-208-460-9.

20. Holland, J. H. *Adaptation in Natural and Artificial Systems: An Introductory Analysis with Applications to Biology, Control, and Artificial Intelligence*. The MIT Press, Cambridge, Massachusetts, USA, 1992, ISBN 978-026-208-213-6.

21. Goldberg, D. *Genetic Algorithms in Search, Optimization and Machine Learning*. Reading, Massachusetts: Addison-Wesley Publishing Company, Massachusetts, USA, 1989, ISBN 978-020-115-767-3

22. Kumar, S.; Kaushal, D.R.; Gosain, A.K. Evaluation of evolutionary algorithms for the optimization of storm water drainage network for an urbanized area. *Acta Geophysica* **2019**, 67(1), 149–165.

23. Berres, S.; Coronel, A.; Lagos, R. Solución numérica de un problema inverso aplicando un algoritmo genético contínuo. *Revista de integración, temas de matemática* **2018**, 36(2), doi:10.18273/revint.v36n2-2018001.

24. Costa, L.H.M.; Castro, M.A.H.; Ramos, H. Utilização de um algoritmo genético híbrido para operação ótima de sistemas de abastecimento de água. *Eng. Sanitária e Ambiental [online]* **2010**, 15(2), 187-196, doi:10.1590/S1413-41522010000200011.

25. Kirkpatrick S.; Gelatt C. D., Vecchi M. P. Optimization by Simulated Annealing. *Science, New Series* **1983**, 220(4598), 671-680, doi:10.1126/science.220.4598.671.

26. Metropolis, N.; Rosenbluth, A.W.; Rosenbluth, M.N.; Teller, A.H.; Teller E. Equation of State Calculations by Fast Computing Machines. *Journal of Chemical Physics* **1953**, 21, 1087, doi:10.1063/1.1699114.

27. Szu, H. & Hartley, R. Fast simulated annealing. *Physics Letters A* **1987**, 122, 157-162, doi:10.1016/0375-9601(87)90796-1.

28. Tsallis C. Possible Generalization of Boltzmann-Gibbs Statistics. *Journal of Statistical Physics* **1988**, 52 479–487, doi:10.1007/BF01016429.

29. Tsallis C.; Stariolo D. A. Generalized Simulated Annealing. *Physica A: Statistical Mechanics and its Applications* **1996**, 233(1–2), 395-406, doi:10.1016/S0378-4371(96)00271-3.

30. Moret, M. A.; Pascutti, P. G.; Bisch, P. M.; Mundim, K. C. Stochastic Molecular Optimization Using Generalized Simulated Annealing. *Journal of Computational Chemistry* **1998**, 19(6), 647-657, doi:10.1002/(SICI)1096-987X(19980430)19:6<647::AID-JCC6>3.0.CO;2-R.

31. Da Silva, D.M. Estudo de Otimização Global com Base na Termoestatística Não-Extensiva. Dissertation presented to the Institute of Physics of the Federal University of Goiás, Goiás, Brasil, 2005, https://posgraduacao.if.ufg.br/p/4155-dissertacoes-2005.

32. De Andrade, M. D.; Mundim, K.C.; Malbouisson, L. A. C. Convergence of the Generalized Simulated Annealing Method with Independent Parameters for the Acceptance Probability, Visitation Distribution, and Temperature Functions. *International Journal of Quantum Chemistry, Special Issue: Proceedings of the XIV Brazilian Symposium of Theoretical Chemistry* **2008**, 108(13), 2392-2397, doi:10.1002/qua.21736.

33. Bernardi, R.C.; Melo, M.C.R.; Schulten, K. Enhanced sampling techniques in molecular dynamics simulations of biological systems. *Biochimica et Biophysica Acta* **2015**, 1850(5), 872-877, doi:10.1016/j.bbagen.2014.10.019.

34. Aquino, A.B.M.; Leal, L.A.; Carvalho-Silva, V.H.; Gargano, R.; Ribeiro, L.A.J.; Cunha, W. F. Krypton-methanol spectroscopic study: Assessment of the complexation dynamics and the role of the van der Waals interaction. *Spectrochimica Acta Part A-Molecular and Biomolecular Spectroscopy* **2018**, 205, 179-185, doi:10.1016/j.saa.2018.06.110.

35. Melo, M.C.R.; Bernardi, R.C.; Fernandes, T.V.A.; Pascutti, P.G. GSAFold: A new application of GSA to protein structure prediction. *Proteins: Structure, Function, and Bioinformatics* **2012**, 80 (9), 2305-2310, doi:10.1002/prot.24120

36. Baggio, A.R., Machado, D.F.S., Carvalho-Silva, V.H, Paterno, L.G., de Oliveira, H.C.B. Rovibrational spectroscopic constants of the interaction between ammonia and metallo-phthalocyanines: a theoretical protocol for ammonia sensor design. Physical Chemistry Chemical Physics **2017**, 19(17), 10843-10853, doi:10.1039/c6cp07900h.

37. Sobrinho, C.A.M., Dias, M.A., Nascimento, C.M.A. Multi-reference Hartree-Fock configuration interaction calculations of LiH and Be using a new double-zeta atomic base. Journal of Molecular Modeling **2014**, 20(8), 2382, doi:10.1007/s00894-014-2382-6.

38. Carroll, D.L. Genetic Algorithms and Optimizing Chemical Oxygen-Iodine Lasers. In *Developments in Theoretical and Applied Mechanics*; Wilson, H., Batra, R., Bert, C., Davis, A., Schapery, R., Stewart, D., Swinson, F., Eds.; School of Engineering, The University of Alabama, USA, 1996; Volume 18, pp. 411-424, ISBN 978-0-96-345891-9.

39. Krishnakumar, K. Micro-Genetic Algorithms for Stationary and Non-Stationary Function Optimization. In Proceedings of the *SPIE: Intelligent Control and Adaptive Systems*, Philadelphia, PA, USA, 1989, 1196; pp. 289-296, doi:10.1117/12.969927

40. Aguero-Martinez, D. S. Evaluation of Genetic Algorithms in Calibration Model of Water Flow in Unsaturated Soil using an Experimental Study. In Proceedings of the "XX Simpósio Brasileiro de Recursos Hídricos", Bento Gonçalves, RS, Brazil, 17-22 November 2013, ISSN 2318-035.

41. Zienkiewicz, O.C. The Finite Element Method, 3rd edition; McGraw-Hill: London, UK, 1977, ISBN 978-0-07-084072-0.

42. Huyakorn, P.S. e Pinder, G.F. Computational Methods in Subsurface flow, 3rd edition; Academic Press: New York, USA, 1983, ISBN 978-0-12-363480-1.

43. Huyakorn, P.S.; Lester, B.H.; Faust, C.R. Finite element techniques for modeling groundwater flow in fractured aquifers. *Water Resources Research* **1984**, 19(4), 1019-1035, doi:10.1029/WR019i004p01019.

44. SURJANOVIC, S.E., BINGHAM, D. (2013). Virtual Library of Simulation Experiments: Test Functions and Datasets. Retrieved June 14, 2021, from http://www.sfu.ca/~ssurjano.